Iranian Journal of Pharmaceutical Research (2016), 15 (2): 403-413
Received: December 2014
Accepted: April 2015

Original Article

The Role of Nanoparticle in Brain Permeability: An *in-vitro* BBB Model

Niusha Nikandish[a,b], Leila Hosseinzadeh[a,b], Abbas Hemati Azandaryani[a] and Katayoun Derakhshandeh[c*]

[a]*Nano Drug Delivery research center, Kermanshah University of Medical Sciences, Kermanshah, Iran.* [b]*Pharmaceutical Sciences Research Center, Faculty of Pharmacy, Kermanshah University of Medical Sciences, Kermanshah, Iran.* [c]*Department of Pharmaceutics, Faculty of Pharmacy, Hamadan University of Medical Sciences, Hamadan, Iran.*

Abstract

Membrane permeability and P-glycoprotein (P-gp) efflux system are regulating factors in the drug brain penetration. Recently, some drug delivery systems have been developed to overcome these limitations. In this study, Metoclopramid has been encapsulated in PLGA nanoparticles using the emulsification/solvent evaporation technique for *in-viro* evaluation of the effect of PLGA nanoparticles on BBB permeability. Subsequently, prepared nanoparticles were characterized using PCS, TEM, FT-IR, DSC and XRD techniques and *in-viro* cell permeability of optimum formulation was evaluated using MDCK cell line as BBB model.

Data investigation showed that prepared nanoparticles have the entrapment efficiency of 50 %. PCS investigation showed that prepared nanoparticles have an average size of approximately 150 ± 14 nm and a relatively monodisperse distribution. TEM micrographs of the samples showed spherical shape and smooth surface with a particle size of nanometric range. Through DSC thermograms and XRD diffractograms analysis, it was demonstrated that there was no crystalline form of the drug in the loaded formulation.

Moreover, our results showed that the greater crossing of metoclopramide in the form of nanoparticle in comparison with the free form. The widely used rhodamine-123 transport assay performed in the MDCK cells demonstrated the presence of P-glycoprotein in this model.

Keywords: Poly (D,L-lactide co glycolide); Blood Brain Barrier;P-glycoprotein; MDCK cell line.

Introduction

P-glycoprotein (P-gp) is a major adenosine triphosphate (ATP) -binding cassette (ABC) transporter responsible for multidrug-resistance (MDR) in the cancer chemotherapy. Until now, the identified ABC proteins are P-gp, breast cancer resistance protein, and multidrug resistance-associated proteins (MRPs) (1). ABC transporters play an important role in the multidrug resistance (MDR), which is often encountered in the acquired immune deficiency syndrome and can certherapy (2, 3). P-gp from ABC transporters exists in different kinds of animals and is considerably manifested in cancer cells that would cause difficulties in cancer therapy. In addition to tumors, P-gp exists in typical tissues such as brain, pancreas, liver, kidney, and colon (4, 5).

The brain is a unique organ that is protected from the periphery organelles by the blood–brain

* Corresponding author:
E-mail: k.derakhshandeh@umsha.ac.ir

barrier (BBB) and the blood–cerebrospinal fluid barrier (BCSFB). The BBB with large surface area (approximately 20 m^2) presents a wide permeability range; therefore, it highly regulates intercellular signaling pathways and maintains CNS homeostasis (6). Several neuropathological conditions such as stroke, bacterial or viral infection, multiple sclerosis, Alzheimer's disease, Parkinson's disease and epilepsy brain tumors can alter the integrity of the BBB and, as a result, CNS permeability can be significantly altered (7). Since the majority of drugs and large molecular weight particulate agents such as recombinant proteins, peptides, monoclonal antibodies (mAb), and gene therapeutics are not readily infused into brain parenchyma due to the BBB limits, permeability of this agent is one of the most significant challenges facing CNS disease treatment (8, 9).

The research conducted in the last decade has frequently demonstrated that drug-transporting from P-gp is so important in the blood–brain barrier. Immunohistochemistry and the analysis of isolated brain capillaries have shown that P-gp exists in the endothelial cells that form the BBB and are functionally active in transporting drugs from the brain (or basolateral) side to the blood (apical or luminal) side of these cells (10). Subsequent analysis of knockout mice lacking P-gp in the BBB and other animal models treated with P-glycoprotein blocking agents demonstrated that *in-vivo* blood–brain barrier P-glycoprotein can prevent the accumulation of many compounds, including a variety of drugs, in the brain (11, 12).

Thus, drug delivery to the brain is one of the many benefits of these carriers and the drug transportation across the BBB is very important for this drug carrier. Recently, some drug delivery systems have been developed to transport drugs across the BBB. One of the most commonly employed systems is nanoparticles fabricated from biocompatible and biodegradable compounds. Since these systems are often polymeric and submicron in size, they can ingeneral be used to provide targeted delivery (cellular/tissue) of drugs to CNS (13-16). Various polymers have been used in drug delivery research for nanoparticles fabrication. Poly (lactide- co- glycolide) acid (PLGA) is a biocompatible and biodegradable polymer that has been used for nanoparticles preparation (14-16).

Research using PLGA has shown that investigating polymer permeability is very important. In this study, metocloperamid loaded PLGA NPs were used for the investigation of polymer effects on the drug transporting from BBB. Then, NP›s characteristics were evaluated using several methods and instruments and the polymer effects on cell membrane were studded by MDCK cell line.

Experimental

Materials

Metoclopramide (MET) was obtained from Sigma (München, Germany) and Poly (lactide-co- glycolide) acid (PLGA; 50:50 MW 12000, inherent viscosity of 0.16–0.24 dl/g) was obtained from the Bohringer Ingelheim Co. (Germany). Polyvinyl alcohol (PVA), Dimethyl sulfoxide (DMSO) and acetone were purchased from Merck (Darmstadt, Germany). All other reagents were available at the highest grade and were obtained from commercial sources.

Preparation of MET loaded nanoparticles

MET loaded polymeric nanoparticles of PLGA were prepared by emulsification/solvent evaporation method. Briefly, the exact polymer and drug amouts were dissolved in acetone and then suspended in the aqueous phase. PVA was employed as a surfactant. The resulting NP suspension was stirred for 3h at room temperature to organic solvent evaporation. Subsequently, the nanoparticles were separated by ultracentrifugation (Beckman, XL-90) at 30,000 rpm for 20min and lyophilized by using a lyophilizer (ZibrusVaco 10-II-E; Germany) to obtain a fine powder of MET loaded NPs.

Determination of Encapsulation efficiency

The percentage of incorporating MET (Encapsulation efficiency, EE) was determined by spectrophotometric determination at 309 nm using a spectrophotometer (Shimadzu, Japan).To do this, 10 mg of NPs powder was dissolved in DMSO and then the absorbance of the samples was measured. The calibration curve

was obtained with this solvent. The drug EE in the PLGA nanoparticles was calculated using the equations (1): (17)

$$EE\ (\%)=\left(\frac{W_a}{W_t}\right)\times 100 \qquad \text{Eq. 1}$$

Where W_t and W_a were the weight of the drug added in the system and analyzed weight of the drug, respectively.

Nanoparticle characterization

The particle size, polydispersity index (PDI), and zeta potential of the NPs were measured by photon correlation spectroscopy (PCS) (Malvern Zetasizer ZS; Malvern, UK). The dried powder samples were suspended in ultra-purified water and slightly sonicated before measurement. Subsequently, the mean diameter, PDI, and zeta potential of the resulted homogeneous suspension were assessed.

The morphology and structure of the nanoparticles were examined by transition electron microscope (Zeiss-EM10C-Germany) at an accelerating voltage of 80 kV capable of point-to-point. Before analysis, the samples were diluted and applied on a carbon-coated grid, and then they were stained with uranyl acetate for 30 seconds and placed on copper grids with films for observation. To obtain a TEM image, the freshly prepared nanoparticles were investigated.

FT-IR characterization of nanoparticles

Fourier transformed-infrared spectroscopy (FT-IR) spectra were obtained using Schimadzu IR-prestige 21 FTIR spectrometer. To measure the FT-IR spectrum of nanoparticles, 2 mg of the samples was mixed with 10 mg KBr and compressed into tablets. The IR spectra of these tablets were obtained in an absorbance mode and in the spectral region of 450 to 4,000 cm^{-1}.

Differential scanning calorimetry (DSC) and X-ray Diffraction Study

DSC experiments were performed in order to characterize the physical state of MET in nanoparticles. Thermograms of the MET, Polymer, nanoparticles, and physical mixtures of drug and polymer were recorded on a DSC-60 (Shimadzu, Japan). Five milligrams of samples were put in an aluminum pan and were hermetically sealed. The heating rate was 10 ^oC/min and the heat flow was recorded from 10- 260 ^oC. The DSC instrument was calibrated for temperature using octadecane and indium. Furthermore, for enthalpy calibration, indium was sealed in aluminum pans with a sealed empty pan as a reference.

In order to determine the drug carrier interaction and physical state of the drug in the state of amorphous or crystalline before and after formulations, XRD study was conducted for the pure drug, polymer, physical mixture, and nanoparticles. XRD patterns were obtained using an X-ray diffractometer-PW1710 (Philips, Holland). The X-ray powder diffraction patterns were obtained at room temperature, voltage of 35 kV and current 20 mA.

In-vitro release study

The *in-vitro* drug release of the MET-loaded NPs was studied by the dialysis membrane method using Franz diffusion cell. Considering the sink condition, 10 mg of suspended nanoparticle in phosphate buffer saline (0.1 M, pH 7.4) was placed on the donor site and 50 mL buffer in receptor chamber was incubated at 37 ^oC under magnetic stirring (400 rpm). At specified time intervals, 2 mL of the medium was taken and replaced with the same volume of fresh buffer. For drug concentration measurement, the taken samples were analyzed at 309 nm using a spectrophotometer. The release results were plotted as the cumulative percentage of the drug content in the dissolution media *vs* time. Each dissolution study was carried out in triplicate.

Experimental Conditions for the BBB Permeability Assay

For the transport studies, MDCK cells (80 % confluent) were seeded at a density of 10^5 cell/mL on the upper side of 12 -well plate filters (1.131 cm^2 growth area, Costar, Cambridge, MA). The culture medium (0.5 mL in the apical side and 1.5 mL in basolateral side) was replaced 3 days following seeding for 2 days.

The quality of the monolayers was assessed by measuring their transepithelial electrical resistance (TEER) at 37 °C using an EVOM epithelial Voltmeter with an Endohm electrode

(World Precision Instruments, INC., Sarasota, FL.). The TEER shows the impedance to the passage of small ions through the physiological barrier and is recognized as one of the most

accurate and sensitive measures of BBB integrity (18). Only monolayers displaying TEER values above 400 Ω were used in the experiments (15).

We pre-incubated the MDCK cell lines at 37 °C in 5% CO_2 conditions for 2 days, establishing strongly reconstructed tight-junctions in the BBB models. TEER was measured to confirm the functionality of the tight-junctions. Our assays were carried out using the BBB cell layers with TEER values in the range of 400 to 2000 Ω cm^2. After establishing that MDCK display extremely tight barrier properties we added nanoparticles, suspended in 0.2 mL assay medium or the free drug to the apical side of the BBB layers and cultured the model for 3, 6, 24 or 48 h and the TEER values were monitored during 24 h.

Functional assay for P-glycoprotein

Activity of P-glycoprotein was determined by the measurement of the polarity of the transport of rhodamine 123, a fluorescent P-gp substrate (19). Breafly, confluent MDCK grown in the 12 well/ plate, were washed with PBS at 37°C, before incubation with 20 μM of the fluorescent P-gp substrate rhodamine 123 (R-123) in the presence of nanoparticles and free drug. Rhodamine 123 in Ringern Hepes buffer was measured for 1 h at 37 °C in the luminal-to-abluminal directions. Rhodamine 123 content was determined by flouresensce microplate reader. (BioTek, USA; excitation wavelength at 485, emission wavelength at 538 nm).

Calculation of permeability coefficient (Papp)

We executed these tests over each period and at the end of the assay, we collected the medium from both the apical and the basolateral sides of the BBB model and we measured the drug concentration in the medium, based on the analytical curves of sample. To evaluate the transportation capacity, we used the apparent permeability coefficient (*P*app), which is calculated by following formula:

$$P_{app} = \frac{dQ}{dt} \times \frac{1}{A C_0}$$

$\frac{dQ}{dt}$ is the transferred drug per time; C_0 initial concentration of fluorescent nanoparticles in apical side; A: surface area of membrane.

Results

Nanoparticles characterization

In the present work, NPs containing MET were prepared by the modified emulsification/solvent evaporation method. The average diameter of 150 nm with PDI lower than 0.3 and an entrapment efficiency of 50 % for PLGA nanoparticles was obtained.

The zeta potential is a key factor for the evaluation of the stability of the NPs suspension. Zeta potential for PLGA NPs was about -11.1 mV that demonstrated the stability of nanoparticles. The negative zeta potential of NPs can rise by a number of means, for example the ionization of chemical groups on the surface or the adsorption of ions (20). The cell membrane has been negatively charged. So when the absolute value of the zeta potential is negative, the circulation half-life of NPs might be increased in blood (21).

TEM images of the prepared NPs showed spherical shape and smooth surface by means of a particle size in nanometric range (Figure 1). The particle size of nanoparticles obtained from TEM images and the results obtained with PCS are the same.

FT-IR Studies

The principle goal in nanoparticles preparation is the complete loading of the drug in the carrier; thus, the investigation of this issue is so important. For this goal, the FT-IR spectrum of pure drug, polymer, physical mixture of drug, and polymer and nanoparticles were obtained as shown in Figure 2. The figure shows that the drug peaks do not exist in the FT-IR spectrum of nanoparticles, while the physical mixture of drug and polymer represent the peaks of drug and polymers.

Differential scanning calorimetry and X-ray Diffraction Studies

The DSC thermograms corresponding to MET, Polymers, physical mixtures, and freeze-

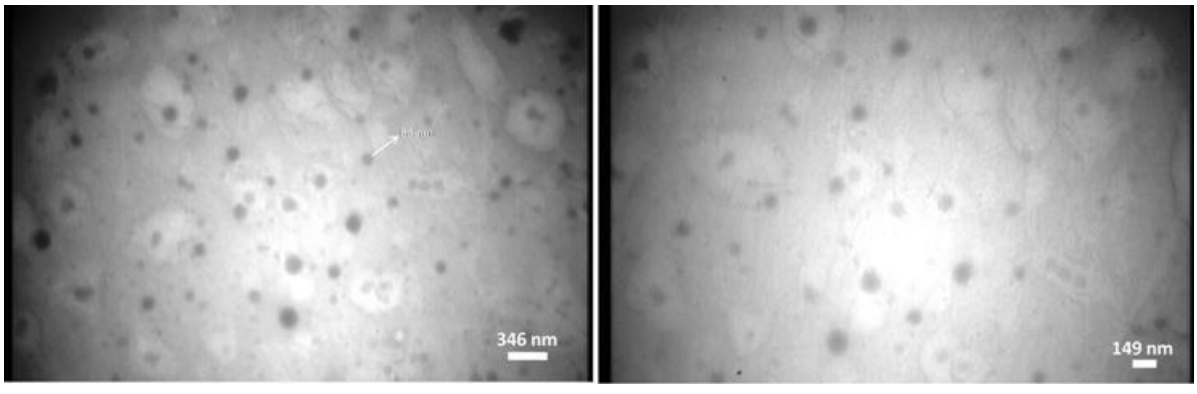

Figure 1. TEM micrographsof PLGA nanoparticles.

dried nanoparticles are shown in Figure 3. The PLGA thermogram displayed an endothermic peak at 45 ^{o}C, corresponding to the polymer transition temperature (Figure 4a). The DSC curve of MET showed an endothermic peak corresponding to its melting point with an on set temperature of 90 °C and a peak of 96 °C. This was confirmed by the presence of a melting peak for MET in the physical mixture. However, there was no distinct MET melting endotherm

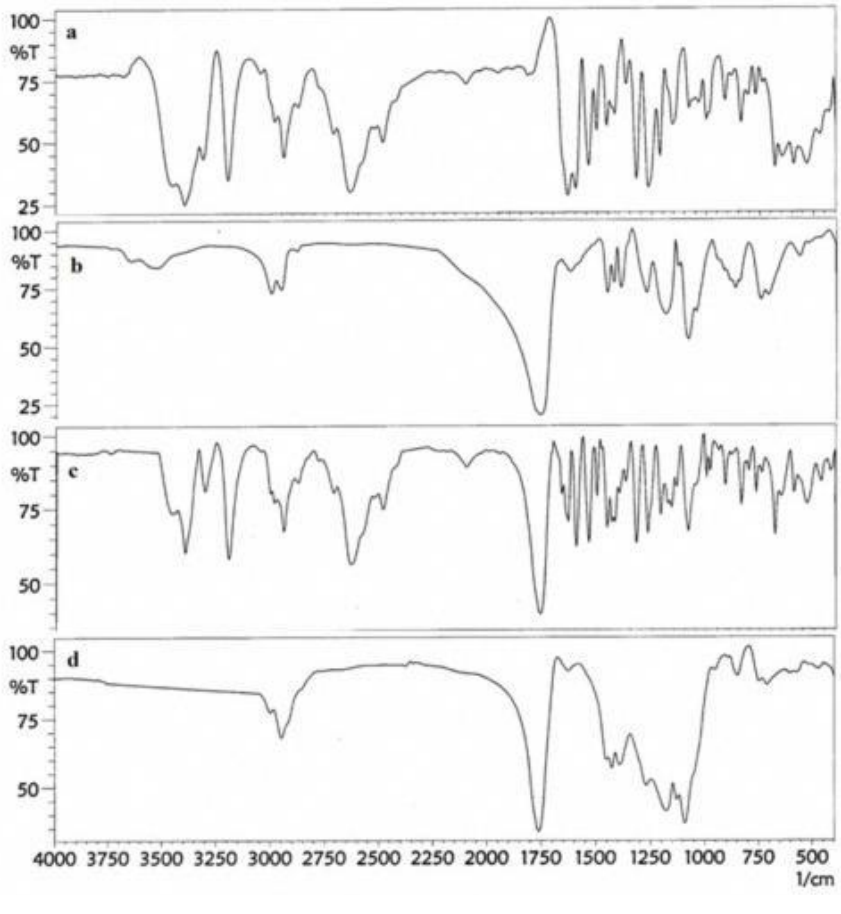

Figure 2. FT-IR peaks of Met powder (a), polymer (b), physical mixtures of drug and polymer (c) and freeze dried nanoparticles (d).

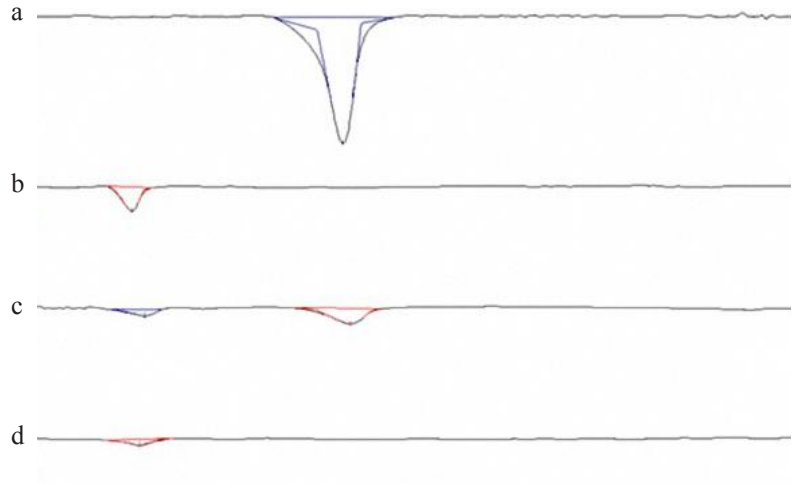

Figure 3. DSC thermograms of Met powder (a), polymer (b), physical mixtures (c) and freeze dried nanoparticles (d)

in the nanoparticles that might be due to the complete amorphization of the drug dispersed in the nanoparticles.

Figure 4 shows the X-ray diffraction patterns of MET, PLGA, the physical mixtures of drug and polymer and nanoparticles. The XRD diffraction patterns of the drug and polymer in physical mixture present multiple peaks, which indicates the presence of free crystalline form of drug and amorphous polymer. The diffraction peak intensity in the MET was similar to the physical mixture while this peak is not shown in the nanoparticles formula. So an amorphous structure was observed for the freeze-dried products indicating complex formation. Similar results were reported for other drugs with the amorphous state loading of the drug (22).

All of the DSC results were in good agreement with those obtained by XRD and FT-IR to prove the encapsulation of drug with nanoparticles.

In-vitro drug release study

It has been reported that the drug release is affected by particle size. The smaller-sized nanoparticles show higher drug release rates. This behavior may be explained by a corresponding increase in surface area to volume ratio, resulting in a larger drug fraction exposed to the medium (17, 23).

Several studies have investigated MET *in-vitro* release characterization (24-26). In the present study the *in-vitro* release profile of MET under sink conditions is summarized in the cumulative percentage release as shown in 5. This figure shows that up to 92 % of the drug was released in the first 10 h. This is due to the solubility of drug and drug diffusion from nanoparticles.

In-vitro cell line study

The cell permeability of MET loaded nanoparticles was evaluated by the MTT assay method on the MDCK cell line after 48 h of exposure to different concentrations of free or encapsulated NPs (Figure 6). As obtained from Figure 6, the drug permeability in the form of encapsulated is three times higher in comparison with free form.

Evaluation of BBB permeability by PLGA nanoparticles

Our results in Figure 7a indicate that nanoparticles decreased the TEER of the BBB model cell line proving that NPs can be opened by the tight junction of BBB. Also the functional activity of Pgp was also tested on this model using rhodamine 123 as a ligand. This indicates the functional expression of P-gp in this *in-vitro* model.

As shown in Figure 7b, the presence of NPs produced a significant increase rhodamine 123 percent in the basolateral side compared to the concentration in the presence of Free drug.

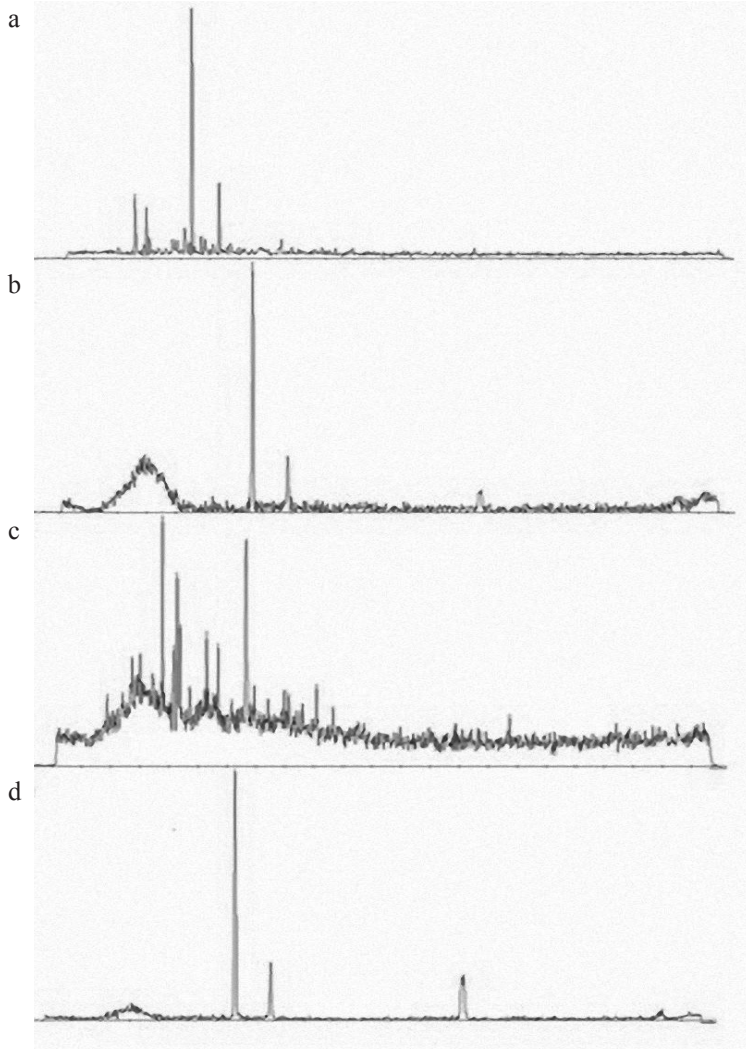

Figure4 . The X-ray diffraction patterns of Met (a), PLGA (b), physical mixture of drug- polymer (c) and nanoparticles (d).

Permeability coefficient (P_{app})

The P_{app} for BBB model was calculated and the amounts of = 3×10^{-4} cm/min and 8.6×10^{-4} cm/min obtained for free drug and PLGA nanoparticles, respectively. As represented, the P_{app} is three times higher when the drug was encapsulated in the PLGA polymer; it has proved the positive effect of PLGA on cell lines permeability.

Discussion

Metoclopramide is a substituted benzamide derivative, structurally similar to procainamide and sulpiride. In behavioral, biochemical, and neuroendocrine tests it displays classic neuroleptic dopamine antagonist properties, which is widely used in the treatment of various gastro intestinal disorders. Preclinical and clinical studies have shown that metoclopramide possesses appreciable central dopamine blocking properties. It causes hyperprolactinaemia like other available neuroleptics and pretreatment with leavodopa inhibits this prolactin response. Antiemetic doses of metoclopramide have been shown to be devoid of antipsychotic therapeutic activity. However, it was demonstrated in an open study that metoclopramide in high doses has significant antipsychotic activity and produced an overall improvement in acute schizophrenic symptoms (27, 28).

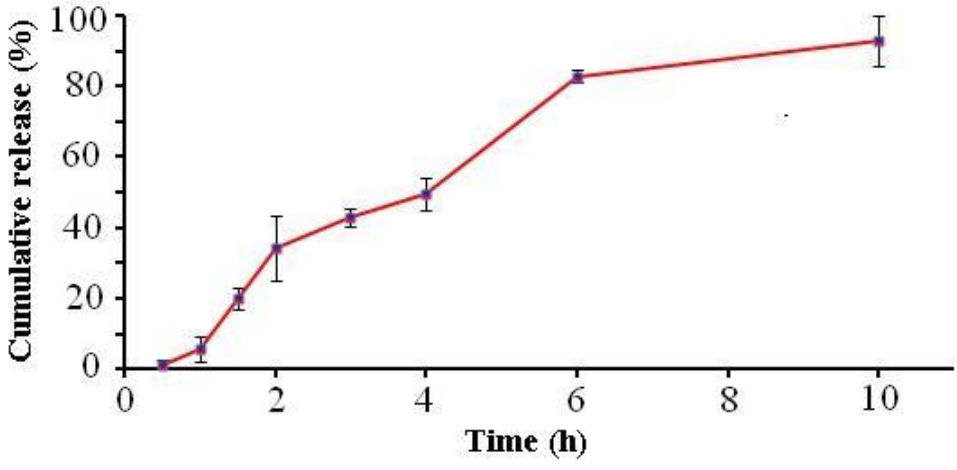

Figure 5. *In-viro* release profile of MET from PLGA nanoparticles in PBS (pH=7.4), the data represent mean ± SD (n=3).

As this drug shows effective antipsychotic effect in high doses and due to low lipophilisity and to be P-gp substrate has low BBB permeability, in this study, we formulated this drug in nanocarrier and evaluate this hypothesis in developed *in-vitro* BBB model.

In this report, we investigated the ability of PLGA nanocarrier in BBB permeability of drug to the brain. As our experiments indicated, this polymer could increase the drug transport in target part of the body.

Madin–Darby canine kidney cell culture mimics certain properties of the blood–brain barrier (BBB). These cells display morphological, enzymatic, and antigenic cell markers found in cerebral endothelial cells and have been reported as a suitable model for this barrier. This cell line was identified as the most promising cell line among several other cell lines for qualitative predictions of brain distribution, and also for distinguishing compounds that pass the blood–brain barrier by passive diffusion and those that are substrates for active efflux of P-gp. Until now, several studies have utilized this drug for carrier evaluation (29-31).

Summerfield et al. investigated drug characterization on the permeability of BBB using *in-vitro* MDCK cell line model. This study showed that the permeability of metoclopramide in the free form is very low; this is the confirmation

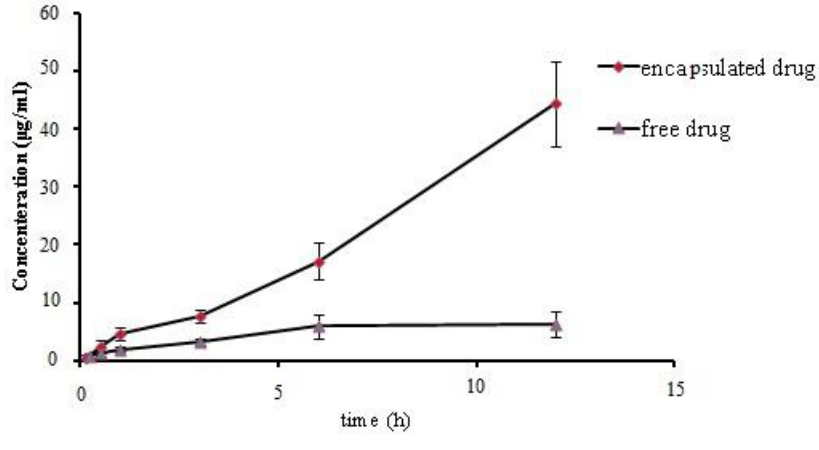

Figure 6. .*In-vitro* cell line permeability investigation using MDCK cell line, the data represent mean ± SD (n=3).

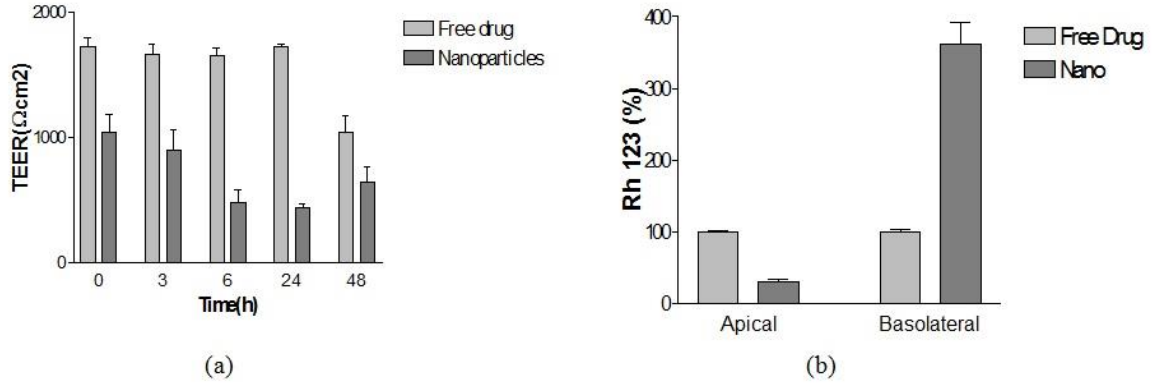

Figure 7. Evaluation of BBB Permeability by PLGA nanoparticles; the effect of nanoparticles and free drug on nanoparticles with TEER measuring (a) and the amount of rhodamine 123 in the apical and basolateral parts of the BBB model after treating with PLGA NPs and free drug

of our results for free drugs In addition the presence of the efflux transporter Pgp was demonstrated in this model. This transporter is important for the nutrient transport and for the extrusion of drugs at the BBB (32, 33).

Rollin and *et al*. investigated the transmission of anticancer drugs from BBB to brain in the form of microparticles of PLGA. This group showed the drug diffuses in the vicinity of the implantation site. Also in this study, it was proved that the microspheres authorized a wide delivery of the drug to the tumor site to inaccessible areas of the brain. Shrinidh and *et al*. investigated rivastigmine-loaded PLGA NPs in *in-vitro* and *in-vivo* conditions. This group showed that the formulation has a good potential for drug diffusing to the brain (34, 35). Finally, from these results and ours, it was proved that PLGA nanoparticles have the ability of drug transporting from BBB. Hence, for further evidence the *in-vivo* experiments must be done.

Conclusion

In the present study, Metcloperamide loaded PLGA nanoparticles were successfully prepared by emulsification/solvent evaporation technique, and the physicochemical characteristics were obtained through an investigation of their properties such as drug loading, morphology, size, and thermal behavior. The obtained nanoparticles had a spherical shape without any aggregation, with the corresponding particle size less than 200 nm.

MET was successfully formulated into NPs, with a small enough size and high absolute zeta potential values and negative surface charges to be suitable for IV injection. TEM micrographs of the nanparticles showed spherical shape with a particle size in nanometric range. The FT-IR spectrums proved the complete loading of the drug in the core of nanoparticles without a Met on the surfaces of particles. From DSC thermograms and XRD analysis diffractograms it was demonstrated that there was no crystalline loading of the drug in the formulation. It represented an amorphous state of drug in the NPs. The *In-vitro* MDCK cell line investigation of the formulations using diffusion cell demonstrated the greater crossing of metoclopramide in the form of nanoparticle in comparison with the free metoclopramide. Further investigation demonstrated that the PLGA nanoparticles do not have destructive effects on the P-gp receptors. Accordingly, we argue that MET-incorporated polymeric nanoparticles of PLGA are a superior candidate for efficient delivery of drug from BBB to the brain.

Acknowledgements

This work was performed in partial fulfillment of the requirements for a Pharm. D of Niusha Nikandish in the Faculty of Pharmacy, Kermanshah University of Medical Sciences Kermanshah-Iran.

References

(1) Loscher W and Potschka H. Drug resistance in brain diseases and the role of drug efflux transporters. *Nat. Rev. Neurosci.* (2005) 6: 591–602.

(2) Eisenblatter T, Huwel S and Galla HJ. Characterization of the brain multidrug resistance protein (BMDP/ABCG2/BCRP) expressed at the blood–brain barrier. *Brain Res*. (2003) 971: 221–231.

(3) Bauer B, Hartz AM, Fricker G and Miller DS. Modulation of p-glycoprotein transport function at the blood–brain barrier. *Exp.Biol. Med*. (2005) 230: 118–127.

(4) Leslie EM, Deeley RG and Cole SP. Multidrug resistance proteins: role of P-glycoprotein, MRP1, MRP2 and BCRP (ABCG2) in tissue defense. *Toxicol. Appl. Pharmacol*. (2005) 204: 216–237.

(5) Kuo YC and Lu CH. Expression of P-glycoprotein and multidrug resistance-associated protein on human brain-microvascular endothelial cells with electromagnetic stimulation. *Colloid Surf B: Biointerfaces* (2013) 9: 57– 62.

(6) Neuwelt EA, Bauer B, Fahlke C, Fricker G, Iadecola C, Janigro D, Leybaert L, Molnar Z, O›Donnell ME, Povlishock JT, Saunders NR, Sharp F, Stanimirovic D, Watts RJ and Drewes LR. Engaging neuroscience to advance translational research in brain barrier biology. *Nat. Rev. Neurosci.* (2011) 12: 169–182.

(7) Zlokovic BV. The blood–brain barrier in health and chronic neurodegenerative disorders. *Neuron* (2008) 57: 178–201.

(8) Pardridge WM. The blood–brain barrier: bottle neck in brain drug development. *Neuro. Rx.* (2005) 2: 3–14.

(9) Wong HL, Wu XY and Bendayan R. Nanotechnological advances for the delivery of CNS therapeutics. *Adv. Drug Deliv. Rev.* (2012) 64: 686–700.

(10) Saija A, Princi P, Trombetta D, Lanza M and De Pasquale A. Changes in the permeability of the blood-brain barrier following sodium dodecyl sulphate administration in the rat. *Exp. Brain Res.* (1997) 115: 546–551.

(11) Schinkel AH. P-Glycoprotein, a gatekeeper in the blood–brain barrier. *Adv. Drug Deliv. Rev.* (1999) 3: 179–194.

(12) Naito M and Tsuruo T. Role of P-glycoprotein in the blood-brain barrier. In: S. Gupta, T. Tsuruo (Eds.), Multidrug Resistance in Cancer Cells, John Wiley and Sons, Ltd., Chichester. (1996) 321–333.

(13) Tsuji A and Tamai I. Blood–brain barrier function of P-glycoprotein. *Adv. Drug Deliv. Rev.* (1997) 25: 287–298.

(14) Derakhshandeh K, Erfan M and Dadashzadeh S. Encapsulation of 9-nitrocamptothecin, a novelanticancer drug, in biodegradable nanoparticles: factorial design, characterization and release kinetics. *Eur. J. Pharm. Biopharm.* (2007) 66*:* 34–41.

(15) Derakhshandeh K, Hochhaus G, Dadashzadeh S. Invitro cellular uptake and transport study of 9-nitrocamptothecin PLGA nanoparticles across Caco-2 cell monolayer model. *Iran J Pharm Res*. (2011) 10(3): 425-234.

(16) Heidarian Sh.,. Derakhshandeh1 K, Adibi3 H., Hosseinzadeh L. Active targeted nanoparticles: Preparation, physicochemical characterization and in vitro cytotoxicity effect. *Res Pharm Sci*. (2015) 10(3): 241-242.

(17) Teixeira M, Alonso MJ, Pinto MM and Barbosa CM. Development and characterization of PLGA nanospheres and nanocapsules containing xanthone and 3-methoxyxanthone. *Eur. J. Pharm. Biopharm.* (2005) 59: 491–500.

(18) Rutten MJ, Hoover RL, Karnovsky MJ. Electrical resistance and macromolecular permeability of brain endothelial monolayer cultures. *Brain Res* (1987) 425: 301−310.

(19) Haseloff RF, Blasig IE, Bauer HC, Bauer H. In search of the astrocyticfactor(s) modulating blood–brain barrier functions in brain capillary endothe-lial cells in vitro. *Cell Mol Neurobiol.*(2005) 25: 25–39.

(20) Mohammadi G, Nokhodchi A, Barzegar-Jalali M, Lotfipour F, Adibkia KH, Ehyaei N and Valizadeh H. Physicochemical and anti-bacterial performance characterization of clarithromycin nanoparticles as colloidal drug delivery system. *Colloids Surf. B: Biointerfaces.* (2011) 88: 39-44.

(21) Sathigari S, Chadha G, Lee P, Wright N, Parsons DL, Rangari VK, Fasina O and Babu RJ. Physicochemical Characterization of Efavirenz–Cyclodextrin Inclusion Complexes. *AAPS. Pharm. Sci. Tech.* (2009) 10: 81-89.

(22) Fernandez-Carballoido A, Pastoriza P, Barica E, Montejo C and Negro S. PLGA/PEG derivativepolymeric matrix for drug delivery system application: characterization and cell viabilitystudies. *Int. J. Pharm.* (2008) 352: 50–7.

(23) Afshari M, Derakhshandeh K and Hosseinzadeh L. Characterization, cytotoxicity and apoptosis studies of methotrexate-loaded PLGA and PLGA-PEG nanoparticles. *J. Microencapsul.* (2014) 31: 239-245.

(24) Hasan EI.Amro BI, Arafat T and Badwan AA. Assessmentof a controlled release hydrophilic matrix formulation for metoclopramide HCl. *Eur. J. Pharm. Biopharm.* (2003) 55: 339–344.

(25) Tas C, Ozkan CK, Savaser A, Ozkan Y, Tasdemir U and Altunay H. Nasal absorption of metoclopramide from different Carbopol 981 based formulations: *In-viro*, *ex-vivo* and *in-vivo* evaluation. *Eur. J. Pharm. Biopharm.* (2006) 64: 246–254.

(26) Abdel-Rahman SI, Mahrous GM and El-Badry M. Preparation and comparative evaluation of sustained release metoclopramide hydrochloride matrix tablets. *Saudi. Pharm. J.* (2009) 17: 283–288.

(27) Doongaji DR, Desai AB, Satoskar RS. Metoclopramide in schizophrenia (an open study). *J. Postgrad. Med*. (1986) 32: 139-145.

(28) Doran A, Scott Obach R, Smith BJ, Hosea NA, Becker S and Venkatakrishnan K. The impact of P-glycoprotein on the disposition of drugs targeted for indications of the centeral nervous system: evaluation

using the MDR1A/1B knockout mouse model drug. *Drug Metab. Dispos*. (2004) 22: 165-174.

(29) Garberg P, Ball M, Borg N, Cecchelli R, Fenart L, Hurst RD, Lindmark T, Mabondzo A, Nilsson JE, Raub TJ, Stanimirovic D, Terasaki T, Oberg JO and Osterberg T. *In-viro* models for the blood–brain barrier. *Toxicol. In-viro.* (2005) 19: 299–334.

(30) NavarroC, González-Álvarez I, González-Álvarez M, Manku M, Merino V, Casabó VG, and Bermejo M. Influence of polyunsaturated fatty acids on cortisol transport through MDCK and MDCK-MDR1 cells as blood-brain barrier *in-viro* model. *Eur. J. Pharm. Sci.* (2011) *42*: 290–299.

(31) Chen ZZ, Lu Y, Du SY, Shang KX and Cai CB. Influence of borneol and muscone on geniposide transport through MDCK and MDCK-MDR1 cells as blood–brain barrier *in-viro* model. *Int. J. Pharm.* (2013) 456: 73– 79.

(32) Summerfield SG, Read K, Begley DJ, Obradovic T, Hidalgo IJ, Coggon S, Lewis AV, Porter RA and Jeffrey P. Central nervous system drug disposition: The relationship between in situ brain permeability and brain free fraction. *J. Pharmacol. Exp. Ther.* (2007) 322: 205–213.

(33) Pardridge WM. Drug and gene targeting to brain with molecular Trojan horses. *Nat. Rev. Drug Discov.* (2002) 1: 131–139.

(34) Roullin VG, Deverre JR, Lemaire L, Hindre´ F, Venier-Julienne MC, Vienet R and Benoit JP. Anticancer drug diffusion within living rat brain tissue: an experimental study using (3H) (6)-5-fluorouracil-loaded PLGA microspheres. *Eur. J. Pharm. Biopharm.* (2002) 53: 293–299.

(35) Shrinidh A, Sandip S and Krutika K. Rivastigmine-loaded PLGA and PBCA nanoparticles: Preparation, optimization, characterization, *in-viro* and pharmacodynamics studies. *Eur. J. Pharm. Biopharm.* (2010) 76: 189-199.

This article is available online at http://www.ijpr.ir